Humidity–Temperature Relationships in the Tropical Troposphere

DE-ZHENG SUN

Program in Atmospheric and Oceanic Sciences, Princeton University, Princeton, New Jersey

ABRAHAM H. OORT

Geophysical Fluid Dynamics Laboratory/NOAA, Princeton, New Jersey

(Manuscript received 10 May 1994, in final form 16 February 1995)

ABSTRACT

Based on the observed interannual variations of water vapor and temperature over the past 26 years the authors have examined the relationship between the variations of water vapor and temperature in the tropical troposphere. The authors find that in both the lower and upper troposphere, tropical mean specific humidity increases with temperature. The rate of fractional increase of specific humidity with temperature at 500 mb is as large as that in the surface boundary layer. However, the rate of fractional increase of specific humidity with temperature is significantly smaller than that given by a model with a fixed relative humidity, particularly in the region immediately above the tropical convective boundary layer. The variations of tropical mean relative humidity show consistently a negative correlation with the temperature variations.

The authors have further compared the spatial structure of the specific humidity variations with that of the temperature variations. Though the vertical structure of tropical mean specific humidity has more variability than that of the tropical mean temperature, the leading EOF for the normalized specific humidity variations is almost exactly the same as the leading EOF for the normalized temperature variations. The characteristic horizontal structure of the specific humidity variations at levels in the free troposphere, however, is very different from that of the temperature variations. The leading EOF for the normalized specific humidity variations at levels in the free troposphere is characterized by regions with alternating positive and negative signs, while the leading EOF for the corresponding temperature variations has a single sign throughout the Tropics. When the variations are averaged zonally, the leading EOF for the normalized specific humidity variations still differs significantly from that of the normalized temperature variations, but the leading EOF has the same sign from the deep Tropics to the subtropics.

1. Introduction

Water vapor plays a dominant role in the radiative budget of the troposphere. It is the principal greenhouse gas and is strongly coupled with clouds. In general circulation models (GCMs), water vapor feedback is the largest response that amplifies the warming induced by the increase of CO_2, and cloud feedback has been identified as the major source of uncertainty (IPCC 1990, 1992). Through its radiative effects and phase changes, water vapor not only plays a key role in atmospheric processes, but also serves as a crucial link between the atmosphere and other components of the climate system (Manabe and Stouffer 1993; Peixoto and Oort 1992). The critical role of water vapor in climate and climate change warrants a thorough attempt to understand its behavior.

Central to the behavior of water vapor in climate change is its relationship with temperature. Unfortunately, this relationship is poorly known in the tropical troposphere. In their pioneering study of the impact of an increase of CO_2 on climate, Manabe and Wetherald (1967) assumed that the relative humidity was constant with temperature. Based on the observational data that were available at that time, they noted that the zonal mean distributions of the relative humidity during winter and summer resemble each other while the zonal mean distributions of specific humidity for the two seasons do not. In fact, the seasonal changes of relative humidity in the Tropics are also large. Figure 1 shows the relative humidity differences between northern summer and northern winter. Only in regions outside the Tropics (defined here as the entire domain of the Hadley circulation, 30°S–30°N), the seasonal changes in relative humidity are small. Since there is little seasonal change of temperature in the Tropics, the changes of relative humidity in the Tropics are mostly due to the seasonal change of the position of the Hadley circulation. Due to the seasonal change of the Hadley circulation, regions with ascending motion in the summer may have descending motion in the winter. Figure 1 simply reflects the fact that the ascending branch of

Corresponding author address: Dr. De-Zheng Sun, National Center for Atmospheric Research, P.O. Box 3000, Boulder, CO 80307-3000.

© 1995 American Meteorological Society

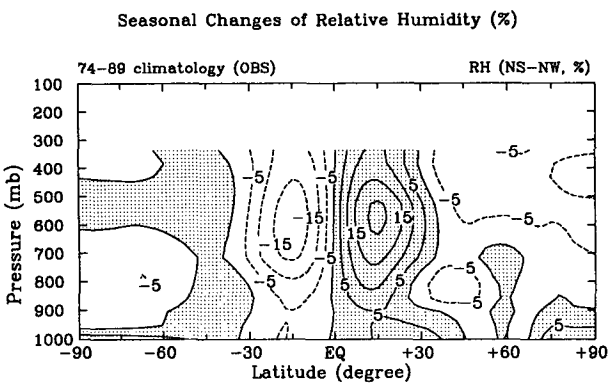

FIG. 1. Relative humidity difference between northern summer (June–August) and northern winter (December–February) (1974 to 1989 climatology). Data are from the global analyzed data archived at GFDL (Oort 1983). Areas with positive values are shaded.

the Hadley circulation is moister than its descending branch.

Theoretical analysis of the moisture budget of the Tropics suggests that the water vapor–temperature relationship in the Tropics may be strongly height dependent (Sun and Lindzen 1993a,b). They proposed a conceptual model for the vertical distribution of water vapor that is characterized by three regions: the tropical convective boundary layer, the free tropical troposphere, and the outflow region of deep convection (see Fig. 10 in Sun and Lindzen 1993a). They argued that the functional dependence of water vapor on temperature in the free troposphere may be significantly different from that in the convective boundary layer.

The observed interannual variations of temperature and humidity offer an opportunity to assess the water vapor–temperature relationship in the tropical troposphere. The interannual variability in the Tropics is largely associated with the El Niño phenomenon. The El Niño phenomenon results in a significant temperature perturbation throughout the free tropical troposphere (Horel and Wallace 1981). In this article, we will use 26 yr of rawinsonde data to examine the relationship between the interannual variations of water vapor and temperature. We are particularly interested in the vertical structure of this relationship. Water vapor feedback (the amplification of the warming induced by the increase of CO_2 due to a concomitant change of water vapor with temperature) depends strongly on the vertical structure of the change of water vapor. It has been found that the water vapor feedback is approximately proportional to the fractional change of water vapor and that changes of water vapor at all heights of the troposphere are important (Shine and Sinha 1991).

The vertical structure of the variability of the temperature and humidity over the tropical western Pacific Ocean has been studied by Gutzler (1992a). He noted that the vertical structure of the decadal trend of specific humidity is distinctly different from the vertical structure of the interannual and seasonal variability. Based on this finding, he further argued that the short-term climate variability of humidity is a poor proxy for the long-term change. The relationship between temperature and humidity exhibited in the interannual or seasonal variations was not examined in his study. Using radiosonde data from 50 stations for 1973–90, Gaffen et al. (1992a) examined the relationship between the total precipitable water vapor W and surface air temperature T_s. They found that over restricted ranges of surface air temperature, the relationship between W and T_s derived from radiosonde data is in good agreement with the relationship between W and T_s from satellite data. They also found that the relationship between W and T_s depends on the timescale and geographical region considered. In their study, they did not examine the vertical structure of the relationship between water vapor and temperature.

In addition to the direct relationship between the variations of water vapor and temperature, we will also examine the spatial structure of the variations of water vapor and temperature using correlation maps and empirical orthogonal functions. In particular, we want to know the relationship between variations of water vapor in the upper troposphere and those in the lower troposphere, and the relationship between variations of water vapor in the deep Tropics and those in the subtropics. A major concern in assessing the nature of water vapor feedback in climate change has been whether the change of water vapor in the upper troposphere follows the change of water vapor in the lower troposphere, and whether the change of water vapor in the subtropics has the same sign as that in the deep Tropics (Lindzen 1990; Betts 1990; Sun and Lindzen 1993a,b). Since our understanding of the temperature structure in the tropical troposphere is relatively better than for moisture (Emanuel 1991; Held and Hou 1981), it is of particular interest to compare the spatial structure of the specific humidity variations with that of the temperature variations. An empirical orthogonal function analysis of three-dimensional variations of humidity has been made by Gaffen et al. (1991). Their focus was on the spatial and temporal scale of the variations of humidity rather than on the relationship between variations of specific humidity in some key regions.

In this paper, we will first discuss the data and methods used for the analysis (section 2). In section 3, we derive the functional dependence of the tropical mean specific humidity on local temperature at all levels in the tropical troposphere. We will see that the vertical structure of this functional dependence differs significantly from that of a model with constant relative humidity. In section 4, we will examine the vertical structure of the tropical mean variations of specific humidity with a focus on the relationship between the variations of specific humidity in the upper troposphere and those

in the lower troposphere. In section 5, we will examine the horizontal structures of variations of specific humidity. Finally, we will summarize our results and discuss their implications in sections 6 and 7.

2. Data and methods

The data are from the global rawinsonde network, analyzed and gridded at GFDL (Geophysical Fluid Dynamics Laboratory) (Oort 1983, updated). The data consist of global monthly mean temperature and specific humidity fields for the period from May 1963 through December 1989.

In deriving the relationship between temperature and humidity, it is desirable to separate the signals that correspond to different physical causes. Thus, we decompose the variations of temperature T and specific humidity q into three parts:

$$T = T_c + T_a + T_l \quad (1)$$

$$q = q_c + q_a + q_l. \quad (2)$$

The subscripts c, a, and l represent, respectively, the normal seasonal cycle, interannual variability, and long-term trend (decadal trend). The physical cause for the long-term trend is less clear than those for the seasonal and interannual variations, but it is unlikely to be the same as that for the interannual variations. We want to extract the relationship between temperature and humidity from variations of T_a and q_a through correlation and regression analysis.

The terms T_a and q_a may be further written as

$$q_a = q_{at} + q_{as} + q_{ar} \quad (3)$$

$$T_a = T_{at} + T_{as} + T_{ar}. \quad (4)$$

The subscripts t, s, and r represent, respectively, the true value, the systematic error, and the random error. Over the interannual timescale, we may assume that T_{as} and T_{ar} are negligible compared to T_{at} and take $T_a = T_{at}$. The terms q_{as} and q_{ar} may not be entirely negligible compared with q_{at}, particularly for the period before 1973 (Gutzler 1992b; Gaffen et al. 1991; Elliott and Gaffen 1991). Fortunately, the temporal variations in q_{as} and q_{ar} are not likely to be correlated with the temporal variations in T_a. Thus, the sign of the correlation coefficient between T_{at} and q_{at} $[C(T_{at}, q_{at})]$ will probably be the same as that between T_a and q_a $[C(T_a, q_a)]$. More importantly, provided that q_{as} and q_{ar} are not correlated with T_a, the functional dependence of q on T derived from variations of T_a and q_a using the least square technique will be the same as that from T_{at} and q_{at}. This further suggests that the errors introduced in the humidity data by instrumental changes may not significantly affect the relationship between temperature and humidity derived through a correlation and regression analysis. The longer the record used to assess the humidity–temperature relationship, the more statistically reliable the relationship derived from the record is. Thus, it is desirable to use the longest record available to assess the relationship between humidity q and temperature T. Unless explicitly mentioned, all calculations presented in this article were made using time series of humidity and temperature that span the entire period (May 1963–December 1989). According to Gaffen et al. (1991), data for humidity after January 1973 are relatively free of errors due to changes in instruments. We will also do our analyses using the data limited to the period January 1973–December 1989. The results will be presented in parallel to the results obtained using the data from the entire period.

To obtain T_a and q_a from T and q, we take T_c and q_c as the climatological mean seasonal values for the period 1964–73. Using the 1964–73 climatology instead of the climatology for the full record is in line with the historical way the rawinsonde data have been analyzed and gridded at GFDL (Oort 1983). For simplicity, we further take T_l and q_l as the linear trend of T and q. When the full record is used for the analysis, T_l and q_l represent the linear trend for the period May 1963–December 1989. When the data for the analysis are limited to the January 1973–December 1989 period, T_l and q_l represent the linear trend for the period January 1973–December 1989. Considering that the decadal trend may not be a sufficiently accurate estimate of the linear trend, we will examine the frequency dependence of our results.

In deriving the relationship between water vapor and temperature, we will use variations of water vapor and temperature averaged over the tropical domain (30°S–30°N). Through horizontal averaging, variations of water vapor and temperature that are related to the horizontal transport by the large-scale circulation will be largely removed, and thus the water vapor and temperature relationship obtained is more indicative of the property of moist convection, and is thus more relevant to the issue of water vapor feedback in global warming [see equations (31), (33), and (29) in Sun and Lindzen 1993a]. As noted by Gaffen et al. (1992b), the regional variability of water vapor in the Tropics is better related to the horizontal transport of the large-scale circulation than the local temperature. To obtain the tropical mean value of temperature and water vapor, it is probably better to use gridded data than station data. The problem of insufficient spatial coverage is reduced by the objective analysis scheme used for interpolating station data onto a regular grid. The objective analysis scheme was designed to minimize the problem of insufficient spatial coverage (Oort 1983; Rosen et al. 1979). We feel it is important, though, to keep in mind that the original spatial data gaps may remain a problem in the gridded data. The spatial coverage of rawinsonde stations over the Tropics is shown in Fig. 2. Plotted in Fig. 2 are the distributions of the rawinsonde stations used in the 500-mb analyses of humidity for January 1973 and January 1983. Note

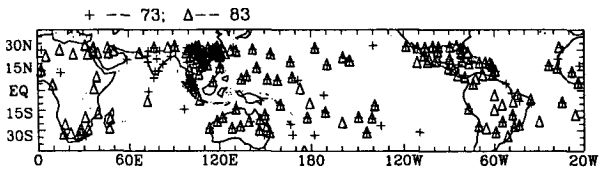

FIG. 2. Distribution of rawinsonde stations used for the analyses of specific humidity at the 500-mb level for January 1973 (+) and January 1983 (Δ).

that the coverage over the eastern Pacific Ocean is relatively poor.

3. Relationship between specific humidity and local temperature

On the interannual timescale, tropical mean temperature and specific humidity have significant and vertically coherent variations. Figure 3 presents time series of variations of q_a and T_a averaged over the entire domain of the Tropics at four representative pressure levels. Temperature variations are plotted as dashed lines. For clarity of presentation, a cosine-bell window (the Hanning window) with a width of seven months was used to slightly smooth the data. The coefficients of this window are given by $h_n = H_n / \sum_1^N H_n$ with

$$H_n = 0.5\left[1 - \cos\left(2\pi \frac{n}{N+1}\right)\right],$$

where $n = 1, 2, \cdots, N$ and N is the width of the window. This smoothing procedure reduces the variance of the temperature and humidity variations by about 10%. Peak anomalies of temperature correspond well with El Niño events. The magnitude of the temperature variations increases with height (from about 0.5 K in the surface boundary layer to 1 K in the upper troposphere). Relative to the local mean specific humidity, the magnitude of the specific humidity variations also increases with height (from about 5% in the surface boundary layer to 10% in the upper troposphere). During most episodes when the temperature has an anomaly peak, the specific humidity also has an anomaly peak of the same sign. A notable exception occurs during the 1982–83 El Niño. During this period, the specific humidity anomalies above 700 mb appear to have the opposite sign of the temperature anomalies. We will discuss possible causes for this exception when we examine the horizontal structure of the variations of humidity in section 5. Overall, the variations of specific humidity correlate positively at all levels with the temperature variations at the same level. However, the strength of the correlation between specific humidity variations and the temperature variations at the same level appears to be strongly height dependent. Figure 4 shows the vertical structure of the correlation coefficients between the mean tropical temperature variations and those in specific humidity. Monthly mean data were used to compute the correlation coefficients. The solid line corresponds to the case in which the entire time series (May 1963–December 1989) are used for the calculations, while the dashed line is for the case in which the data before January 1973 are not included. Note that the strongest correlations occur in the lower and upper troposphere. The correlations in the middle troposphere are much weaker. At 700 mb, the correlation coefficient between T_a and q_a derived from the data limited to the period January 1973–December 1989 is significantly smaller than that from the time series spanning the entire period. Since the length of the data for obtaining the dashed line is much shorter than that for the solid line, the differences between the solid line and the dashed line are not necessarily due to problems in the data before 1973. The vertical structure of the two curves in Fig. 4 is quite similar.

To further quantify the dependence of q on T, we have calculated the rate of change of q with $T(dq/dT)$ using a linear regression. Note that since the magnitude of T_a is small (about 1 K), we may write $q_a = T_a^{-1} dq/dT$. (Assuming that the functional depen-

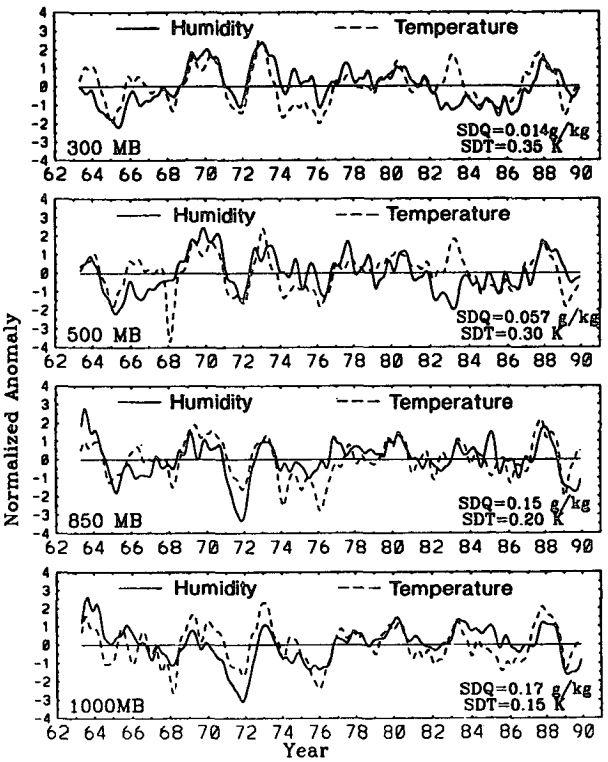

FIG. 3. Time series of the mean tropical (30°S–30°N) temperature (dashed line) and specific humidity (solid line) at four representative pressure levels. The seasonal cycle and linear trend have been removed from each series. A Hanning window with a width of seven months was used to smooth the data. Each series was further normalized by its standard deviation. The standard deviation for each series is given in the lower right-hand corner of the figure (SDQ is for the specific humidity and SDT for the temperature).

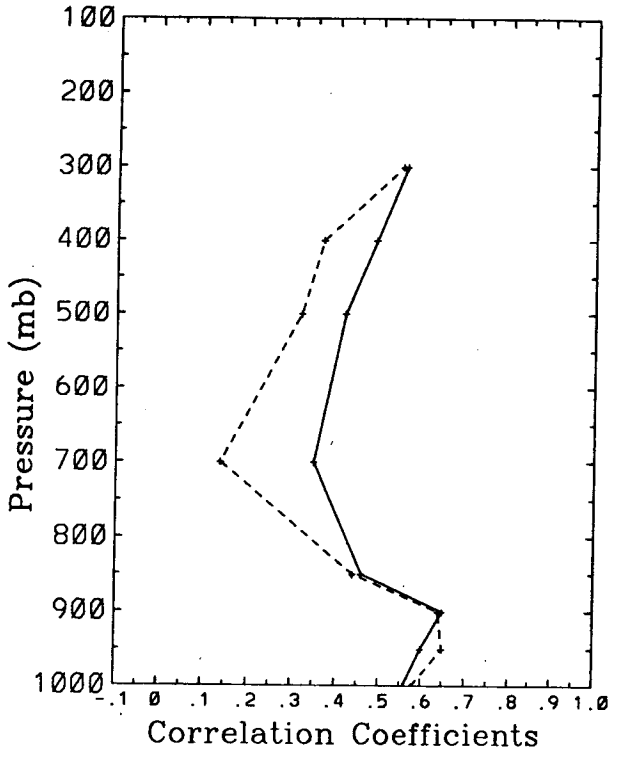

FIG. 4. Vertical structure of the correlation between the variations of tropical mean specific humidity and tropical mean temperature at the same level. Solid line: May 1963–December 1989. Dashed line: January 1973–December 1989.

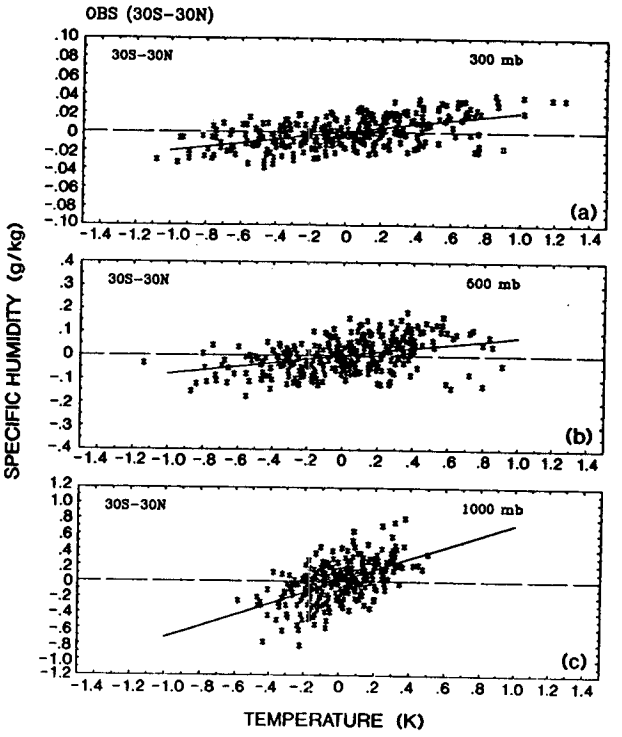

FIG. 5. Scatter plots of variations of tropical mean temperature T_a and specific humidity q_a variations. The solid straight line is a linear regression. Top: 300 mb; middle: 500 mb; bottom: 1000 mb.

dence of q on T is not stronger than for the case of a constant relative humidity, it can be shown that the higher-order terms in the Taylor expansion of q are negligible as long as the deviation of the temperature from the mean is not larger than 1.5 K.) Figure 5 shows scatter diagrams for tropical mean T_a and q_a at three representative levels. These diagrams show that a linear relationship between T_a and q_a is a good fit to the data. Table 1 summarizes the results at various standard pressure levels in the troposphere. Also presented in Table 1 is the rate of change of specific humidity given by a fixed relative humidity model $\mathrm{RH}_c\, dq^*/dT$, where RH_c is the climatological annual mean relative humidity averaged over the tropical domain, and q^* is the saturation specific humidity at the climatological annual mean temperature averaged over the tropical domain. The tropical mean relative humidity is from the climatology for the period 1974–89. The tropical mean temperature is from the 1963–73 climatology. Note that at all levels dq/dT is smaller than $\mathrm{RH}_c\, dq^*/dT$. However, a better indicator of the greenhouse effect of water vapor is the fractional change of water vapor with temperature (Shine and Sinha 1991). Thus, we show in Fig. 6 the vertical structure of the rate of fractional change of q with T (i.e., dq/dT divided by the long-term mean value of specific humidity q_c, where q_c is obtained by averaging the 320 months of data of specific humidity for the period May 1963–December 1989). The rate of fractional change of q with T corresponding to a fixed relative humidity is also plotted in the figure $[q^{*-1}(dq^*/dT)]$. Note that this quantity is independent of the mean relative humidity that is specified. An interesting feature of Fig. 6 is that relative to the climatological mean specific humidity, the largest

TABLE 1. The rate of change of tropical mean specific humidity with tropical mean temperature (30°S–30°N). Results obtained using the full record (May 1965–December 1989) and the data limited for the later period (January 1973–December 1989) are both presented. Presented also in the table is the rate of change of specific humidity with temperature when the relative humidity is fixed at the climatological value ($\mathrm{RH}_c\, dq^*/dT$). See text for the definition of RH_c and q^*.

	dq/dT (10^{-1} g kg^{-1} K^{-1})		
Pressure	May 1963–December 1989	January 1973–December 1989	$\mathrm{RH}_c\, dq^*/dT$ (10^{-1} g kg^{-1} K^{-1})
300	0.21 ± 0.02	0.18 ± 0.02	0.23
400	0.51 ± 0.05	0.34 ± 0.06	0.64
500	0.8 ± 0.1	0.6 ± 0.1	1.3
700	1.4 ± 0.2	0.5 ± 0.3	3.3
850	3.5 ± 0.4	2.9 ± 0.4	6.1
900	5.9 ± 0.4	5.0 ± 0.4	7.1
950	5.6 ± 0.4	5.4 ± 0.4	8.2
1000	7.2 ± 0.6	6.3 ± 0.6	9.5

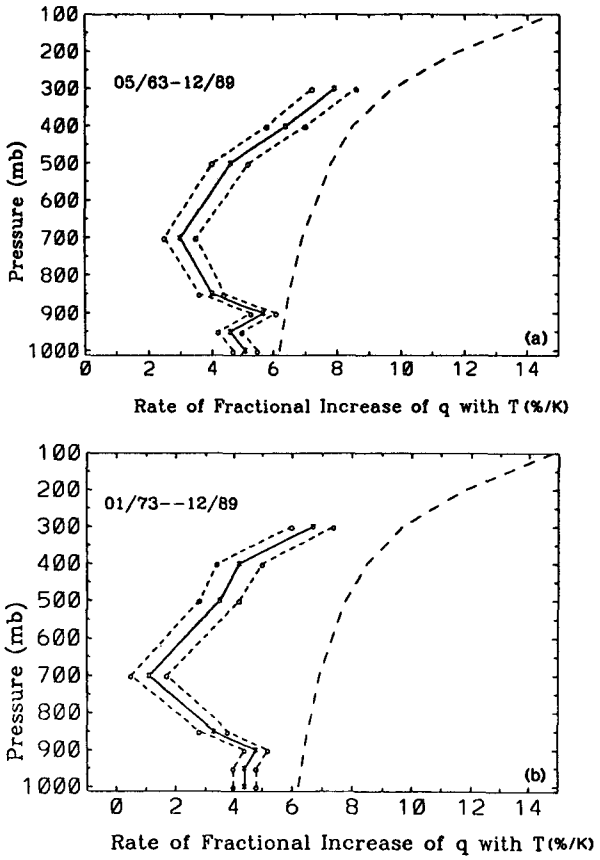

FIG. 6. Vertical structure of the rate of fractional increase of the tropical specific humidity with temperature (solid line, in units of % K^{-1}). The two short-dashed lines are error estimates. For reference, the rate of fractional increase of specific humidity with temperature corresponding to a fixed relative humidity is also plotted in the figure (long-dashed line). Upper: data for the entire period May 1963–December 1989 were used for the calculations. Lower: data for the period January 1973–December 1989 were used for the calculations.

rates of change of q with T occur in the upper troposphere and in the surface boundary layer. The water vapor in the region right above the tropical convective boundary layer has the weakest dependence on the local temperature. Also note that above 500 mb, there is a tendency for the observed rate of change to approach that for a constant relative humidity. It is shown in Sun (1992) that the strong dependence of the rate of evaporation from the ocean on the relative humidity tends to keep the relative humidity in the surface boundary layer constant. In the free troposphere, the subsiding air is primarily moistened by evaporation from hydrometeors falling from upper-level clouds (Sun and Lindzen 1993a). The amount of hydrometeors is probably not sufficient to keep the relative humidity close to a constant, perhaps with the exception of the outflow region of deep convection where there exist widespread clouds. Thus, it appears that the vertical structure of the functional dependence is consistent with the conceptual picture put forward by Sun and Lindzen (1993a).

Note that by the definition of the relative humidity, we have

$$\frac{1}{rh}\frac{drh}{dT} = \frac{1}{q}\frac{dq}{dT} - \frac{1}{q^*}\frac{dq^*}{dT}.$$

Since

$$\frac{1}{q}\frac{dq}{dT} \sim \frac{1}{q_c}\frac{dq}{dT},$$

the difference between the solid line $[q_c^{-1}\,dq/dT]^{-1}$ and the long-dashed line $[q^{*-1}(dq^*/dT)]$ in Fig. 6 gives a measure of $1/rh(drh/dT)$. We see that $1/rh(drh/dT)$ is negative at all levels. Thus, Fig. 6 implies that the rate of increase of the water vapor greenhouse effect with surface temperature (or the water vapor feedback) in the tropical region is considerably smaller than that in an atmosphere with constant relative humidity. Using a radiative-transfer model in which the lapse rate is fixed at the climatological value for the Tropics, we have estimated that the rate of increase of clear-sky greenhouse effect G with temperature (dG/dT). The term G is defined as the difference between the surface emission and the net outgoing longwave radiation at the top of the atmosphere (Raval and Ramanathan 1989). We find that dG/dT corresponding to a fixed distribution of relative humidity [using the same distribution as used in Manabe and Wetherald (1967)] is about 3.8 W K^{-1}. When we replace the assumption of ($drh/dT = 0$) in the region between 1000 mb and 300 mb by the values of drh/dT implied by Fig. 6a, we find that dG/dT decreases to 3.0 W K^{-1}. The radiation code used for this calculation was designed by M. D. Chou (Chou et al. 1991). The climatological values for the tropical lapse rate are from McClatchey et al. (1972).

Figure 6 further implies a negative correlation between the temperature variations and the variations of the relative humidity. We have also calculated directly the correlations between the interannual variations of tropical mean temperature and tropical mean relative humidity (RH), and find that the correlations are negative at all levels. As done for the variations of specific humidity, the variations of relative humidity can also be decomposed into three parts: $RH = RH_c + RH_a + RH_l$. The subscripts c, a, and l represent, respectively, the normal seasonal cycle, interannual variability, and decadal trend. Figure 7 presents the vertical structure of the correlation coefficients between T_a and RH_a, and dRH/dT derived using a linear regression technique. The time series for temperature and relative humidity used to obtain Fig. 7 are for the period May 1973 through December 1989 for which objectively analyzed, monthly averaged relative humidity data are available. The 1974–89 climatology was used to remove the seasonal cycle. The largest anticorrelation between

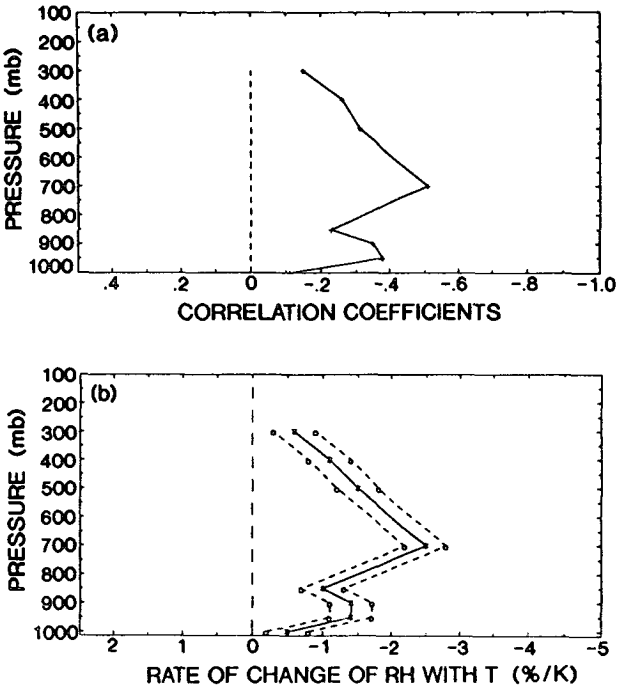

FIG. 7. (a) Vertical structure of the correlation between the variations of the tropical mean temperature and relative humidity. Note that the horizontal axis is reversed from the conventional direction. (b) Vertical structure of the rate of change of relative humidity with temperature. The two dashed lines are error estimates.

T_a and RH_a occurs at 700 mb. The peak value of dRH/dT also occurs at 700 mb, where dq/dT differs most from RH_c dq^*/dT. The values are largely consistent with what is implied by Fig. 6. Note that due to nonlinearity, the monthly values obtained by averaging the daily values (as used here) may differ somewhat from the relative humidity directly calculated from the monthly mean temperature and specific humidity.

To examine whether the above results are frequency dependent, we have redone the above calculations using data filtered by a reversed Hanning window with a width of 121 (10 yr). (Window coefficients are given by $1 - H_n$. Signals with a period longer than 10 yr are largely removed by this window.) The results are almost the same.

4. Vertical structure of the water vapor variations

The major source of moisture is at the ocean surface. We have a very limited understanding of how water vapor is transported upward. In this section, we will examine the vertical structure of the variations of humidity and compare it with the vertical structure of the temperature variations.

a. Relationship between the upper-tropospheric humidity and lower-tropospheric humidity

In the last section, we show that the dependence of specific humidity on local temperature above 500 mb is as strong as in the surface boundary layer. However, correlations between variations of specific humidity in the upper troposphere with those at the surface are quite weak, despite a strong correlation between variations of temperature in the upper troposphere with those at the surface. (Throughout this article, we refer to the 1000-mb level as the surface.) Figure 8 shows the correlations of the variations at all levels with those at the surface. Figure 8a is for the specific humidity and Fig. 8b for the temperature. Figure 8a shows that the correlations of variations of specific humidity at all levels with those at the surface are positive. However, the correlations decrease rapidly with height, and only a small percentage of the variations above the 500-mb level can be explained by the variations in the boundary layer. In contrast, correlations of temperature with those at the surface level remain almost constant with height (Fig. 8b).

The comparatively weak correlations in Fig. 8a seem to be related to very low frequency signals in the specific humidity data. We have found that the correlations of the variations of specific humidity in the free troposphere with those in the convective boundary layer in-

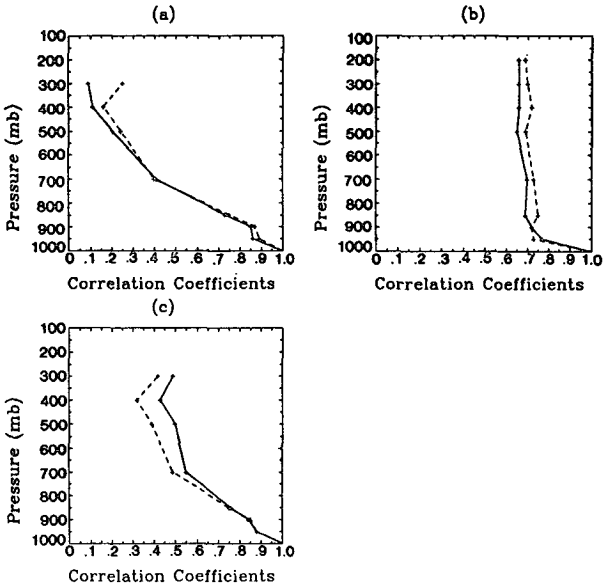

FIG. 8. (a) Vertical structure of the correlation of variations of specific humidity with those at 1000 mb. Solid line: data for the entire period May 1963–December 1989 were used for the calculation. Dashed line: data were limited to the period January 1973–December 1989. (b) Vertical structure of the correlation of variations of temperature with those at 1000 mb. Solid line: data for the entire period May 1963–Dec 1989 were used for the calculation. Dashed line: data were limited to the period of January 1973–December 1989. (c) Vertical structure of the correlation of variations of specific humidity q with those at 1000 mb. Correlations were obtained using filtered data in which variations with a period greater than a decade were largely removed. See text for more details. Solid line: data for the entire period May 1963–December 1989 were used for the calculations. Dashed-line: data were limited to the period of January 1973–December 1989.

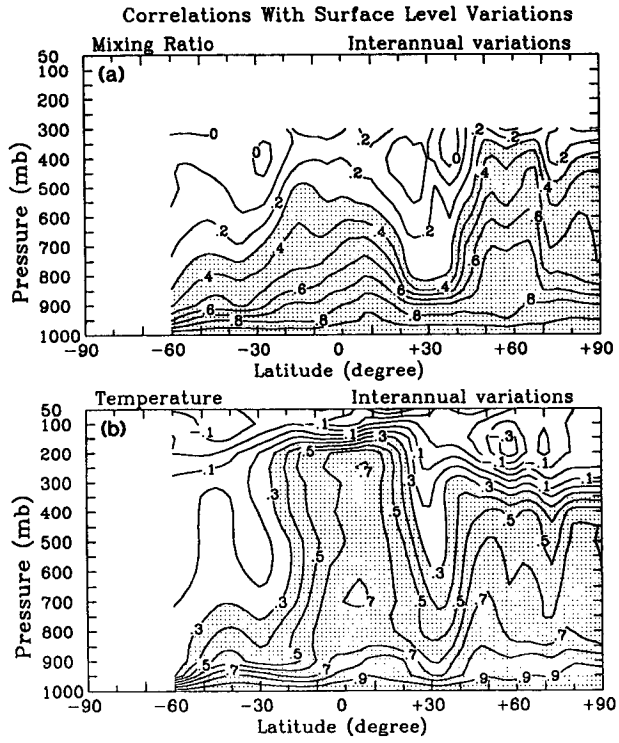

FIG. 9. (a) Cross section of the correlations of the zonal mean specific humidity variations with those at the surface. (b) Cross section of the correlations of the zonal mean temperature variations with those at the surface.

crease significantly when the data are filtered by a reversed Hanning window with a width of 121 (10 years) (Fig. 8c). In contrast, when the low-frequency signals are removed from the temperature data using the same window, the correlations of the temperature variations in the free troposphere with those in the convective boundary layer are almost the same as those obtained using the unfiltered data.

Correlations with surface-level variations can be a good indicator of the mixing effects of moist convection. Figure 9 shows the latitudinal dependence of the correlations between the zonally averaged variations of specific humidity (a) and temperature (b) at all levels with those at the surface (1000 mb). The values calculated for the extratropical regions are also presented for comparison. Areas with a correlation coefficient greater than 0.3 are shaded. Both figures show similar patterns. The correlation coefficients tend to reach maximum values in the deep Tropics and in the middle-latitude eddy regime. Due to the existence of large-scale subsidence over the subtropical regions, the variations at these latitudes in the free troposphere are effectively decoupled from those at the surface. The patterns are consistent with the meridional distributions of zonal mean precipitation and latent heat release as shown in Peixoto and Oort (1992). Note that in the deep Tropics, correlations of variations of temperature with those at the surface are almost constant throughout the depth of the entire troposphere, while correlations of specific humidity variations with those at the surface level decrease quickly with height. When the time series for the specific humidity are filtered by a reversed Hanning window with a width of 10 yr, the correlations in the deep Tropics are noticeably improved (Fig. 10a).

The relationship of specific humidity with local temperature is also a function of vertical mixing. Presented in Fig. 10b is a cross section of the correlations between the variations of specific humidity and temperature at the same height and latitude. Weakest correlations are found in the subtropics. Figures 10a and 10b indicate that over regions where the variations of specific humidity in the free troposphere have a poor correlation with those at the surface level, the variations of specific humidity also have a poor correlation with the temperature variations at the same location.

The above analysis shows that the relationship between variations of the specific humidity in the upper troposphere and those at the surface appears to change somewhat when the lowest frequencies are removed. In the next section, we will use empirical orthogonal function (EOF) analysis to decompose the vertical structure of the specific humidity variations into orthogonal modes (EOFs). The structure of the leading

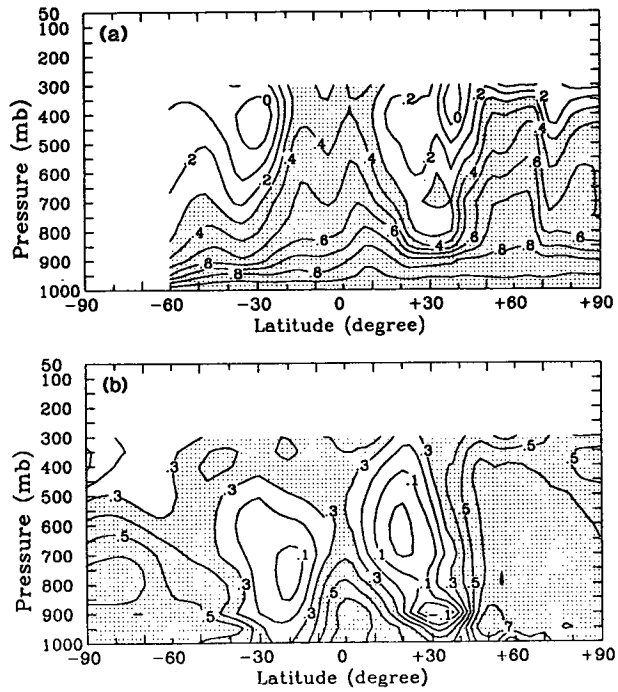

FIG. 10. (a) Cross section of the correlations of the zonal mean specific humidity variations with those at the surface after very low frequency contributions were filtered out by using a reversed Hanning window with a width of 10 yr. (b) Cross section of the correlations between the zonal mean specific humidity variations and the corresponding temperature variations at the same latitude and height.

modes and their corresponding time series will help us to gain more insight into the physical processes involved in determining the relationship between variations of specific humidity in the upper troposphere and those in the lower troposphere.

b. *An EOF analysis of the vertical structure of variations of specific humidity*

An EOF analysis identifies the most preferred modes of the variability and isolates the timescales that are associated with those modes (see Kutzbach 1967 for a more precise mathematical description of EOFs). Since we are mainly interested in the phase relationship of the variations at different levels, we first normalize the variations at each level by their standard deviation. Let f_n be a vector that contains the normalized q_a (or T_a) at all vertical levels for a particular month. The dimension of f_n (M) is equal to the total number of data points (i.e., the total number of vertical levels in this case). We obtain the correlation matrix $\mathbf{R} = \mathbf{F}\mathbf{F}^{\mathrm{T}}$, where $\mathbf{F}$ is a $M \times N$ matrix that contains f_n for all months ($n = 1, 2, \cdots, N$). The EOFs for $\mathbf{F}$ are just the eigenvectors of the matrix $\mathbf{R}$. In Fig. 11, we present the first two leading EOFs for the vertical structure of the variations of specific humidity and temperature averaged over the entire Tropics. The spatial pattern depicted by the first EOF can be regarded as the most preferred or the most characteristic spatial pattern of the variability. Figure 11a shows the first two EOFs for the variations of specific humidity, and Fig. 11b the corresponding EOFs for the variations of temperature. The first two leading EOFs for the normalized specific humidity variations have the same structure as those for the temperature variations. The first EOF is almost constant with height. The second EOF is characterized by a sign reversal roughly at the top of the convective boundary layer (800 mb). The first EOF for both the specific humidity and temperature variations explains the major portion of the total variance. The percentage variance values explained by the first two leading EOFs for humidity are 61% and 26%, and for temperature 79% and 9%, respectively. Thus, it appears that the vertical structure of humidity has more significant modes of variability than the vertical structure of temperature. Note that for a moist adiabatic atmosphere, the temperature variations at all levels of the troposphere should be in phase, and the first EOF would then explain the total variance. If in addition the relative humidity is fixed, the variations of specific humidity throughout the troposphere should also have the same sign so that the leading EOF would also explain the total variance of specific humidity.

The time series corresponding to the first and second EOFs are plotted in Fig. 12a for the specific humidity variations and in Fig. 12b for the temperature variations. These time series are obtained by projecting f_n onto the first and second EOFs. Note that the time

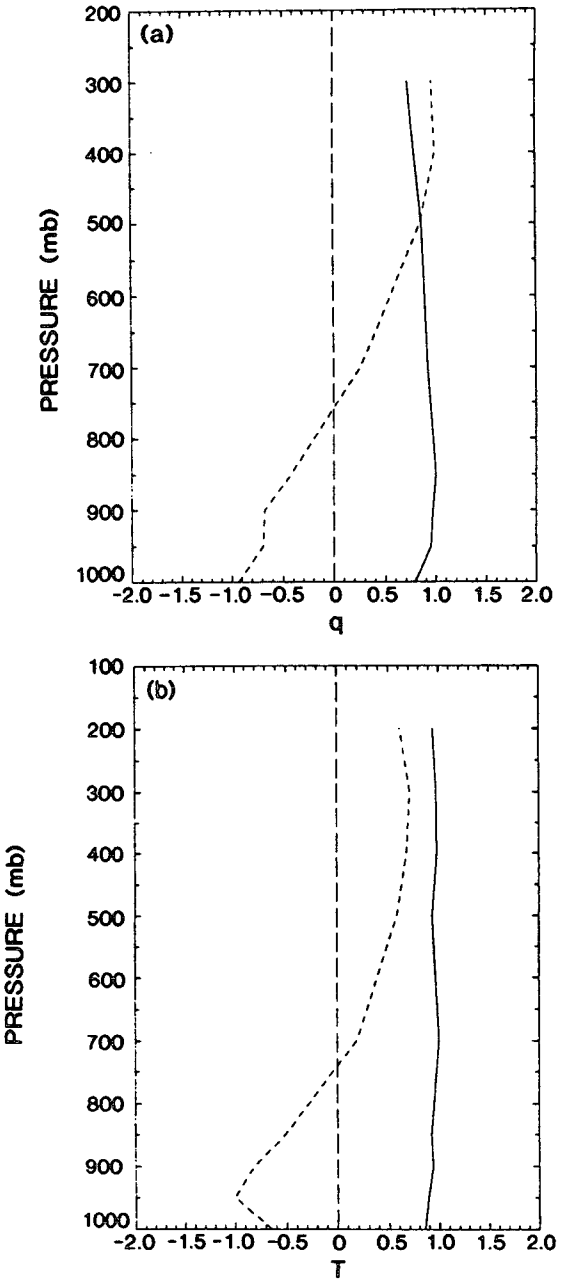

FIG. 11. The first (solid) and second (dashed) EOFs for the normalized specific humidity (a) and temperature (b) variations.

series corresponding to the first EOF is dominated by the El Niño–Southern Oscillation (ENSO) timescale. It is well known that ENSO is associated with dramatic spatial shifts in the tropical convective systems and that it enhances the communication between the free troposphere and the convective boundary layer in some of the more arid regions such as the east Pacific Ocean. With strong vertical mixing, variations at different levels tend to have the same phase. Thus, the first mode represents the effects of vertical mixing by deep con-

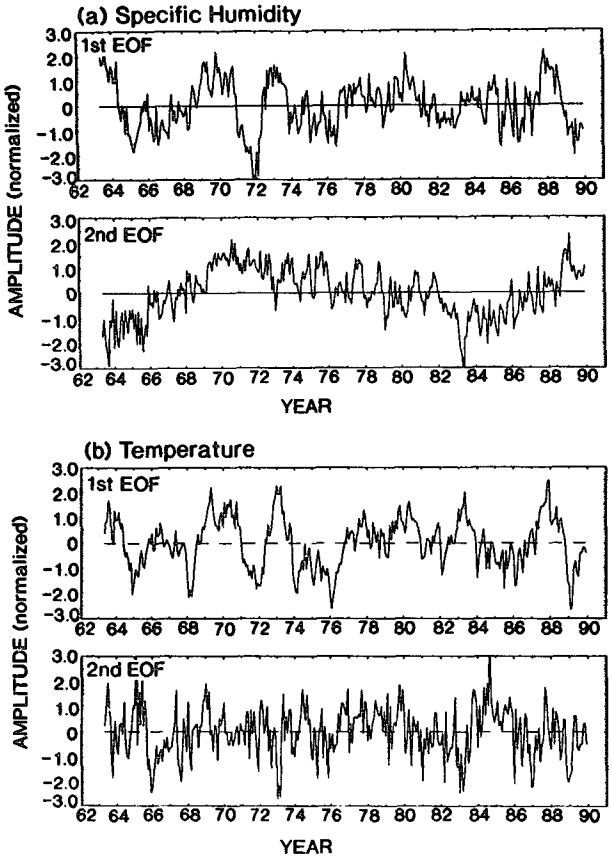

FIG. 12. Time series corresponding to the first and second EOFs for the normalized specific humidity (a) and temperature variations (b). Each series has been normalized by its standard deviation.

vection. The percentage of the variance explained may be regarded as a measure of the mixing effect.

Another interesting feature of Fig. 12a is that the time series corresponding to the second EOF for the specific humidity variations is modulated by a very low frequency signal. Apparently, there is no such signal in the time series for the temperature variations (see Fig. 12b). The physical origin of this signal is not clear. However, systematic errors in the measurements due to instrumental changes may give such a spurious, very low frequency signal after the data are averaged over a large area. When a reversed Hanning window with a width of 121 was used to suppress the very low frequency variations, the variance explained by the first EOF was significantly increased. Thus, it appears that the relatively weak correlations between the variations in the upper free troposphere and those at the low levels may result from a negative correlation between the two series over very long timescales.

When the humidity data for the above analysis are limited to the period January 1973 to December 1989, the first and second EOFs for the specific humidity variations are very nearly the same as shown in Fig. 11. In this case, the percentage variance explained by the first two EOFs are 59% and 16%, respectively.

The above analysis shows that over the El Niño timescale, the variations of the specific humidity in the upper troposphere more or less follow the variations in the lower troposphere. There is no evidence that the enhanced convection associated with the occurrence of El Niño tends to dry the upper troposphere. However, an out-of-phase relationship between the variations in the upper troposphere and those in the lower troposphere may occur over the decadal timescale. In the following section, we will examine the role of the Hadley and Walker circulations in the interannual variability of the tropospheric humidity.

5. Horizontal structure of variations of water vapor

Figure 13 shows the leading EOF for the normalized zonal mean variations of specific humidity (Fig. 13a) and the leading EOF for the normalized zonal mean variations of temperature (Fig. 13b). The EOF for the specific humidity variations accounts for 28% of the total variance, while the leading EOF for the temperature variations explains 42% of the total variance (When the data for the calculation are limited to January 1973 through December 1989, the EOF for the specific humidity has the same pattern with 26% variance explained.) This again shows that there are more significant modes of variability in the specific humidity

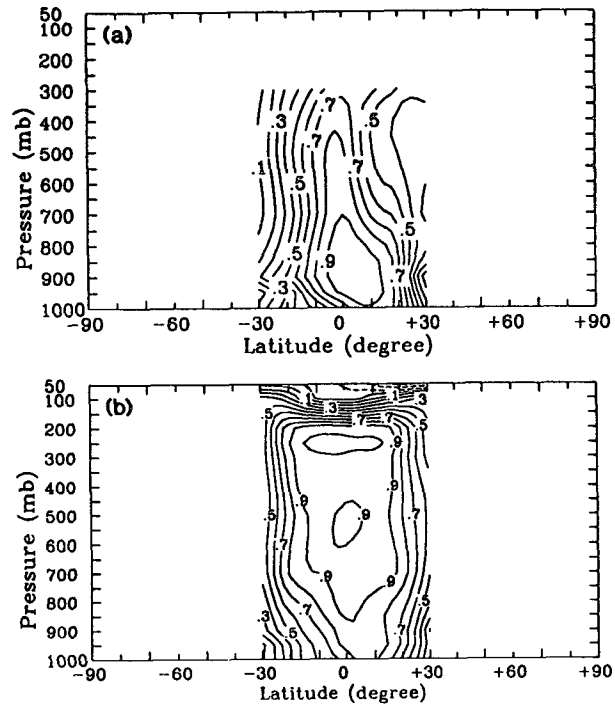

FIG. 13. Leading EOF of the normalized zonal mean variations of specific humidity (a) and temperature (b).

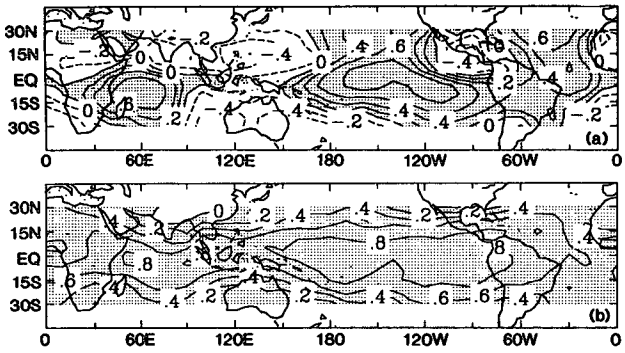

FIG. 14. Leading EOF of the normalized variations of specific humidity and temperature at 500 mb. Top: specific humidity; bottom: temperature.

field. Since interannual variations are mostly associated with ENSO, it is not surprising to see that the centers of action for both the temperature and humidity variations (i.e., the maximum value) are located in the deep Tropics. The leading EOF for the temperature and humidity variations has the same sign throughout the entire tropical domain, indicating that variations in different regions tend to be in phase. However, the spatial pattern of the first EOF for specific humidity (Fig. 13a) shows that the influence of the center of action decays quickly away from the center. In contrast, the spatial pattern of the first EOF for the variations of temperature (Fig. 13b) shows that variations throughout the tropical domain are in unison.

Figure 14 shows a global map of the first EOF for the normalized variations of specific humidity (a) and temperature (b) at the 500-mb level. The variations at each data point are normalized by their standard deviation. All areas with positive values are shaded. The percentage of variance explained by the first EOF is 10% in the case of specific humidity (Fig. 14a) and 30% for temperature (Fig. 14b). When the data for the calculation were limited to the period January 1973 through December 1989, very similar results were obtained. A salient feature in Fig. 14 is that the leading EOF for specific humidity is characterized by regions with alternating positive and negative sign, while the leading EOF for temperature has almost everywhere a positive sign. The spatial pattern of the leading EOF for temperature simply reflects the fact that significant temperature gradients cannot be maintained in the tropical belt due to the efficient heat transport by waves (Gill 1982). The spatial pattern of the leading EOF for specific humidity suggests a correspondence with the ENSO phenomenon. The positive anomalies over the east Pacific Ocean are accompanied by negative anomalies in the west Pacific region. Similar spatial patterns for the variations of water vapor were also found in the three-dimensional EOF analysis by Gaffen et al. (1991). Note that in their analysis, the long-term trend was not removed from the data, and consequently the first EOF from their analysis does not correspond to the ENSO signal, but represents the spatial pattern of the long-term trend. The second EOF from their analysis resembles our Fig. 14a. Note also that in their analysis, specific humidity anomalies at four levels (surface level, 850 mb, 700 mb, and 500 mb) were concatenated into one array and were not normalized.

Figure 15 shows two snapshots of the spatial distribution of the specific humidity anomalies at 500 mb for periods that correspond to the 1982–83 El Niño and the 1972–73 El Niño, respectively. As in Fig. 14a, the two snapshots show that the anomalies over the eastern Pacific Ocean have the opposite sign of those over the western Pacific Ocean. However, the negative anomalies over the west Pacific region for December 1982–February 1983 have a much larger amplitude and cover a much larger area than those for December 1972–February 1973. The positive anomalies in the east Pacific region for December 1982–February 1983 also have a larger amplitude than those of December 1972–February 1973. As a consequence, the decrease of water vapor over the west Pacific region outweighs the increase over the east Pacific region, which leads to a net decrease of water vapor in the upper-tropical troposphere. This probably explains the exceptional relationship between the tropical mean specific humidity and tropical mean temperature shown earlier

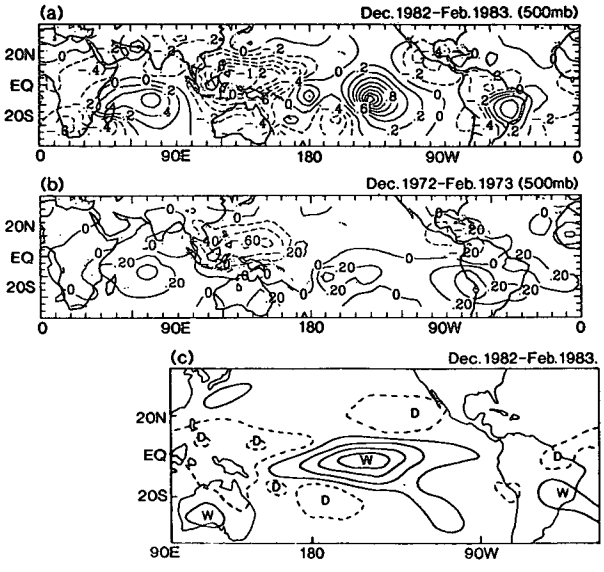

FIG. 15. (a) Spatial distribution of the specific humidity anomalies q_a at 500 mb for December 1982–February 1983; anomalies are in units of g kg^{-1}. (b) Spatial distribution of the specific humidity anomalies q_a at 500 mb for December 1972–February 1973; anomalies are in units of g kg^{-1}. (c) Spatial distribution of the outgoing longwave radiation (OLR) anomaly over the Pacific Ocean (contour interval of 20 W m^{-2}). The anomaly fields are for December 1982–February 1983. Negative anomalies in OLR are indicated by solid lines (labeled W for "wet") and correspond to regions of enhanced precipitation. Positive anomalies in OLR are indicated by dashed lines (D for "dry"). The bottom figure is adapted from Rasmusson and Wallace (1983).

in Fig. 3. The features in Fig. 15a are qualitatively consistent with observations of surface precipitation (Philander 1989). Figure 15c shows the anomaly field of total outgoing longwave radiation (OLR) for December 1982–February 1983 over the Pacific Ocean. A negative anomaly in OLR represents enhanced deep convection. We see that the geographical distribution of specific humidity anomalies in the upper troposphere is consistent with the OLR anomaly field. The specific humidity field has positive anomalies over regions with enhanced deep convection and negative anomalies over regions with decreased deep convection. However, the positive anomalies over the eastern Pacific region may have been underestimated due to the poor data coverage over that region (see Raval et al. 1994). During the 1982–83 El Niño, the region of tropical storm genesis moved far eastward from its normal position. Consequently, the underestimation of the positive anomalies over the eastern Pacific Ocean for the 1982–83 El Niño period could be considerable. Note that in the objective analysis scheme used by Oort (1983), the zonal average of the available data was used as the initial-guess field. Thus, the exceptional relationship between the tropical mean specific humidity anomaly and the tropical mean temperature anomaly for this period could be partially related to the poor coverage over the eastern Pacific Ocean (Raval et al. 1994). For the same reason, the negative correlations between the eastern Pacific Ocean and the western Pacific Ocean shown in Fig. 14 may have been underestimated.

When the very low frequency signals are suppressed by the use of a reversed Hanning window with a width of 121, the leading EOF for the horizontal structure of the specific humidity variations and the explained variance remain almost the same.

6. Summary of major results

Using 26 yr of recent radiosonde data, we have examined the relationships between the interannual variations of temperature and water vapor. We have also compared the spatial structure of the specific humidity variations with that of the temperature variations.

a. Relationship with local temperature

We find that the variations of tropical mean specific humidity at each level of the troposphere have a positive correlation with the temperature variations at the same level (Figs. 3 and 4). In a statistical sense, this implies that water vapor increases with temperature in both the lower and upper troposphere. We have further obtained the rate of increase of specific humidity with temperature through a regression technique. We find that relative to the mean specific humidity, the rate of change of specific humidity with temperature in the upper troposphere is as large as that in the surface boundary layer. The weakest dependence of water vapor on local temperature occurs in the region immediately above the tropical convective boundary layer (800–500 mb). However, the rate of fractional increases at all levels is smaller than that given by a model in which the relative humidity is kept fixed (Fig. 6). The variations of tropical mean relative humidity show consistently a negative correlation with the temperature variations (Fig. 7). The largest decrease of tropical mean relative humidity with the increase of temperature also occurs in the region immediately above the tropical convective boundary layer.

b. Relationships between variations of water vapor in different regions

Compared with the correlations between the variations of tropical mean temperature in the upper troposphere and those at the surface, the connection between the tropical mean specific humidity variations in the upper troposphere and those at the surface is weak. The weak correlations between variations of specific humidity in the upper troposphere and those in the lower troposphere are related to a signal with a period about 10 yr whose vertical structure has a sign reversal at about 800 mb. An EOF analysis shows that to the first order and on the El Niño timescale, the variations of tropical mean specific humidity at different levels are in phase, which indicates effective mixing of water vapor in the vertical.

It is in the horizontal direction that the spatial structure of normalized specific humidity variations differs significantly from that of normalized temperature variations. The changes of specific humidity at 500 mb are characterized by regions with different signs and have a clear correspondence with the ENSO signal. The variations of zonal mean specific humidity in the subtropics are only weakly related to the variations in the deep Tropics.

7. Final remarks

Raval and Ramanathan (1989) were probably the first to use observational data to determine the nature of water vapor feedback in global warming. They examined the relationship between sea surface temperature and the infrared flux at the top of the atmosphere for clear-sky conditions. They derived the relationship from the geographical variations of sea surface temperature and the infrared flux at the top of the atmosphere. The relationship indicates a positive correlation between sea surface temperature and column-integrated water vapor amount (see also Raval et al. 1994; Gaffen et al. 1992a). However, whether the tropospheric water vapor content at all levels is positively correlated with the sea surface temperature is not clear. More importantly, the air must be subsiding in clear-sky regions. When there is large-scale subsidence, the influence from the sea is restricted to a shallow bound-

ary layer, and the free tropospheric water vapor content and temperature are physically decoupled from the sea surface temperature underneath. Thus, it may be questionable to attribute the relationships obtained in such a way to the properties of moist convection.

Using SAGE II (Stratospheric Aerosol and Gas Experiment) data, Rind et al. (1990) examined the seasonal variability of water vapor in selected tropical regions and found that changes in the tropospheric water vapor are positively correlated with changes in the tropospheric temperature. However, a problem with their analyses is that the Hadley circulation shifts seasonally, and consequently what they basically compared are the differences between the ascending region and the descending region of the Hadley circulation. Their analysis did not show what will happen to the Hadley circulation as a whole when the Tropics are warmer or colder than normal.

The results of the present study are not subject to the above criticism because the water vapor–temperature relationship is derived from the interannual variations of tropical mean temperature and humidity. Thus, our present results should be a better indicator of the properties of moist convection and more relevant to the issue of water vapor feedback in global warming. However, we must caution against accepting interannual variability as a surrogate for long-term climate change without further studies. The interannual variability studied here is largely associated with the El Niño phenomenon, which is associated with unstable air–sea interactions (Philander 1989). The perturbations in the atmosphere caused by the air–sea interactions are not necessarily the same as those induced by the increase of greenhouse gases. Gutzler (1992a) noted that the vertical structure of the interannual changes of humidity over the western Pacific Ocean is different from the vertical structure of the decadal trend during the past two decades. We find that the vertical structures of the interannual changes of tropical mean humidity and temperature also differ significantly from those of the corresponding decadal trends. However, one has to be cautious about the reliability of the long-term trend of humidity because of potential problems in the data. Although the water vapor–temperature relationship may not be sensitive to the spatial distribution of the temperature perturbation, this has not been demonstrated explicitly. The longer the timescale, the more physical processes will be involved, such as connections with temperature changes outside the tropical region associated with oceanic variability or aerosol forcing. Thus, the statistical relationships obtained here from the interannual variability may not be used directly to determine the humidity changes in long-term climate variations, such as those due to global warming associated with the increase of greenhouse gases. Nevertheless, the behavior of water vapor in long-term climate change is unlikely to be completely independent of its behavior for the short-term fluctuations, because the same physical processes that are embodied in the interannual variations must also play a role in the long-term climate change.

More importantly, the present results offer an observational basis for checking the results from theoretical and numerical studies of the water vapor–temperature relationship. Given the large feedback of water vapor in GCM calculations of global warming, validating and improving the water vapor–temperature relationship in GCM simulations are of obvious importance. Clearly, if the interannual variations of humidity and temperature simulated by GCMs exhibit the same relationship and spatial structure as we have found here in observations, we can have more confidence in GCM predictions of global warming. The water vapor–temperature relationship and the spatial structures of the temperature and humidity variations simulated by GFDL GCMs will be presented in a subsequent paper.

Acknowledgments. This research has greatly benefited from discussions with Drs. L. Donner, I. Held, J. Lanzante, N.-C. Lau, C. Lindberg, R. S. Lindzen, J. Mahlman, S. Manabe, R. Ramaswamy, and B. Soden. We also would like to thank Dr. D. S. Gutzler and two anonymous reviewers for their helpful comments. The first author (DZS) is particularly grateful to Drs. Held and Mahlman for their advice and support. He also would like to express his gratitude to Professor R. S. Lindzen for his continuing encouragement.

REFERENCES

Betts, A. K., 1990: Greenhouse warming and the tropical water vapor budget. *Bull. Amer. Meteor. Soc.*, **71**, 1465–1467.

Chou, M. D., D. P. Krats, and W. Ridgway, 1991: Infrared radiation parameterizations in numerical climate models. *J. Climate*, **4**, 424–437.

Elliot, W. P., and D. J. Gaffen, 1991: On the utility of radiosonde archives for climate studies. *Bull. Amer. Meteor. Soc.*, **72**, 1507–1520.

Emanuel, K. A., 1991: A scheme for representing cumulus convection in large-scale models. *J. Atmos. Sci.*, **48**, 2313–2335.

Gaffen, D. J., T. P. Barnett, and W. P. Elliott, 1991: Space and time scales of global tropospheric moisture. *J. Climate*, **6**, 989–1008.

——, W. P. Elliott, and A. Robock, 1992a: Relationships between tropospheric water vapor and surface temperature as observed by radiosondes. *Geophys. Res. Lett.*, **19**, 1839–1842.

——, A. Robock, and W. P. Elliott, 1992b: Annual cycles of tropospheric water vapor. *J. Geophys. Res.*, **97**, 18 185–18 193.

Gill, A. E., 1982: *Atmosphere-Ocean Dynamics.* Academic Press, 662 pp.

Gutzler, D. S., 1992a: Climatic variability of temperature and humidity over the tropical western Pacific. *Geophys. Res. Lett.*, **19**, 1595–1598.

——, 1992b: Uncertainties in climatological tropical humidity profiles: Some implications for estimating the greenhouse effect. *J. Climate*, **6**, 978–982.

Held, I. M., and A. Y. Hou, 1981: Nonlinear axially symmetric circulations in a nearly inviscid atmosphere. *J. Atmos. Sci.*, **37**, 515–533.

Horel, J. D., and J. M. Wallace, 1981: Planetary-scale atmospheric phenomena associated with the Southern Oscillation. *Mon. Wea. Rev.*, **109**, 813–829.

IPCC, 1990: *Climate Change: The IPCC Scientific Assessment.* Cambridge University Press, 365 pp.

——, 1992: *Climate Change: The Supplementary Report to The IPCC Scientific Assessment.* Cambridge University Press, 198 pp.

Kutzbach, J., 1967: Empirical eigenvectors of sea-level pressure, surface temperature and precipitation complexes over North America. *J. Appl. Meteor.*, **6,** 791–802.

Lindzen, R. S., 1990: Some coolness concerning global warming. *Bull. Amer. Meteor. Soc.*, **71,** 1465–1467.

McClatchey, R. A., R. W. Fenn, J. E. A. Selby, F. E. Volz, and J. S. Garing, 1972: *Optical Properties of the Atmosphere.* 3d ed., 108 pp.

Manabe, S., and R. T. Wetherald, 1967: Thermal equilibrium of the atmosphere with a given distribution of relative humidity. *J. Atmos. Sci.*, **24,** 241–259.

——, and R. J. Stouffer, 1993: Century-scale effects of increased atmospheric CO_2 on the ocean-atmosphere system. *Nature,* **364,** 215–218.

Oort, A. H., 1983: *Global Atmospheric Circulation Statistics, 1958–1973.* NOAA Professional Paper 14, NOAA, U.S. Dept. of Commerce, 180 pp.

Peixoto, J. P., and A. H. Oort, 1992: *Physics of Climate.* American Institute of Physics, 520 pp.

Philander, S. G. H., 1989: *El Niño, La Nino, and the Southern Oscillation.* Academic Press, 293 pp.

Rasmusson, E. M., and J. M. Wallace, 1983: Meteorological aspects of the El Nino/Southern Oscillation. *Science,* **222,** 1195–1202.

Raval, A., and V. Ramanathan, 1989: Observational determination of the greenhouse effect. *Nature,* **342,** 758–761.

——, A. H. Oort, and V. Ramaswamy, 1994: Observed dependence of outgoing longwave radiation on sea surface temperature and moisture. *J. Climate,* **7,** 807–821.

Rind, D., E. W. Chiou, W. Chu, J. Larsen, S. Oltmans, J. Lerner, M. P. McCormick, and L. McMaster, 1991: Positive water vapor feedback in climate models confirmed by satellite data. *Nature,* **349,** 500–503.

Rosen, R. D., D. A. Salstein, and J. P. Peixoto, 1979: Variability in the annual fields of large-scale atmospheric water vapor transport. *Mon. Wea. Rev.*, **107,** 26–37.

Shine, K. P., and A. Sinha, 1991: Sensitivity of the Earth's climate to height dependent changes in the water vapor mixing ratio. *Nature,* **354,** 382–384.

Sun, D. Z., 1992: Tropical tropospheric water vapor budget, maintenance of the lapse rate, and distribution of the extra-tropical tropospheric temperature and wind. Ph.D. thesis, Massachusetts Institute of Technology, 203 pp.

——, and R. S. Lindzen, 1993a: Distribution of tropical tropospheric water vapor. *J. Atmos. Sci.*, **50,** 1643–1660.

——, and ——, 1993b: Water vapor feedback and the ice-age snowline record. *Ann. Geophys.*, **11,** 204–215.